Accepted Manuscript

An efficient numerical method for singularly perturbed time dependent parabolic 2D convection–diffusion systems

C. Clavero, J.C Jorge

Please cite this article as: C. Clavero and J.C. Jorge, An efficient numerical method for singularly perturbed time dependent parabolic 2D convection–diffusion systems, *Journal of Computational and Applied Mathematics* (2018), https://doi.org/10.1016/j.cam.2018.10.033

An efficient numerical method for singularly perturbed time dependent parabolic 2D convection-diffusion systems

C. Clavero and J.C Jorge

Department of Applied Mathematics and IUMA, University of Zaragoza
Zaragoza, Spain, clavero@unizar.es
Department of Computational and Mathematical Engineering and ISC
Universidad Pública de Navarra, Pamplona, Spain, jcjorge@unavarra.es

Abstract

In this paper we deal with solving efficiently 2D linear parabolic singularly perturbed systems of convection-diffusion type. We analyze only the case of a system of two equations where both of them feature the same diffusion parameter. Nevertheless, the method is easily extended to systems with an arbitrary number of equations which have the same diffusion coefficient. The fully discrete numerical method combines the upwind finite difference scheme, to discretize in space, and the fractional implicit Euler method, together with a splitting by directions and components of the reaction-convection-diffusion operator, to discretize in time. Then, if the spatial discretization is defined on an appropriate piecewise uniform Shishkin type mesh, the method is uniformly convergent and it is first order in time and almost first order in space. The use of a fractional step method in combination with the splitting technique to discretize in time, means that only tridiagonal linear systems must be solved at each time level of the discretization. Moreover, we study the order reduction phenomenon associated with the time dependent boundary conditions and we provide a simple way of avoiding it. Some numerical results, which corroborate the theoretical established properties of the method, are shown.

Key words: parabolic systems, fractional implicit Euler, splitting by components, upwind scheme, Shishkin meshes, uniform convergence, order reduction
PACS: 65N05, 65N12, 65M06, 65N06

1 Introduction

In this work we consider two dimensional time dependent singularly perturbed convection-diffusion systems of type

$$\begin{cases} \mathcal{L}_\varepsilon(t)\mathbf{u} \equiv \dfrac{\partial \mathbf{u}}{\partial t}(\mathbf{x}, t) + \mathcal{L}_{\mathbf{x},\varepsilon}(t)\mathbf{u}(\mathbf{x}, t) = \mathbf{f}(\mathbf{x}, t), \ (\mathbf{x}, t) \in Q \equiv \Omega \times (0, T], \\ \mathbf{u}(\mathbf{x}, t) = \mathbf{g}(\mathbf{x}, t), \ (\mathbf{x}, t) \in \partial\Omega, \times [0, T], \ \mathbf{u}(\mathbf{x}, 0) = \boldsymbol{\varphi}(\mathbf{x}), \ \mathbf{x} \in \Omega, \end{cases} \quad (1)$$

where $\mathbf{u} = (u_1, u_2)^T, \mathbf{x} \equiv (x, y), \Omega = (0, 1)^2$ and the spatial differential operator $\mathcal{L}_{\mathbf{x},\varepsilon}(t)$ is defined as

$$\mathcal{L}_{\mathbf{x},\varepsilon}(t)\mathbf{u} \equiv -\mathcal{D}\Delta\mathbf{u} + \mathcal{B}_x(\mathbf{x})\frac{\partial}{\partial x}\mathbf{u} + \mathcal{B}_y(\mathbf{x})\frac{\partial}{\partial y}\mathbf{u} + \mathcal{A}(\mathbf{x}, t)\mathbf{u}, \quad (2)$$

with $\mathcal{D} = \mathrm{diag}(\varepsilon, \varepsilon), \mathcal{B}_x(\mathbf{x}) = \mathrm{diag}(b_{x,11}(\mathbf{x}), b_{x,22}(\mathbf{x})), \mathcal{B}_y(\mathbf{x}) = \mathrm{diag}(b_{y,11}(\mathbf{x}), b_{y,22}(\mathbf{x}))$ and $\mathcal{A}(\mathbf{x}, t) = (a_{kr}(\mathbf{x}, t)), \ k, r = 1, 2$.

We assume that $0 < \varepsilon \leq 1$ and it can be very small; moreover, the coefficients of the convection matrices satisfy $b_{z,kk}(\mathbf{x}) \geq \rho > 0, \ k = 1, 2, z = x, y$, and the reaction matrix $\mathcal{A}$ is an M-matrix, i.e., it holds

$$\sum_{r=1}^{2} a_{kr} \geq 0, \ k = 1, 2, \ a_{kr} \leq 0, \ \text{if} \ k \neq r, \forall(\mathbf{x}, t) \in \overline{Q}.$$

In order to assure that the exact solution $\mathbf{u} \in C^{4,2}(\overline{Q})$, we suppose that the data $\mathbf{f}(\mathbf{x}, t) = (f_1, f_2)^T, \mathbf{g}(\mathbf{x}, t) = (g_1, g_2)^T, \boldsymbol{\varphi}(\mathbf{x}) = (\varphi_1, \varphi_2)^T$, the convection matrices $\mathcal{B}_z, \ z = x, y$ and the reaction matrix $\mathcal{A}$, are composed by sufficiently smooth functions which, besides, satisfy sufficient compatibility conditions among them (see [12] for a detailed discussion.

The construction and analysis of efficient numerical schemes to solve coupled systems of singularly perturbed problems has received great interest in the recent years. For instance, the case of systems of 1D convection-diffusion elliptic problems is considered in [1,13,14,16], where a coupling in the reaction terms is considered for problems with equal or different diffusion parameters at each equation of the system. In [18], a case of coupling in the convective terms, with equal diffusion parameters was analyzed. For 2D problems, diffusion-reaction systems were studied in [2,6,10,11] for the case of equal diffusion parameters or in [20] for the case of different diffusion parameters. In [15], an elliptic 2D system of convection-diffusion type was considered. Nevertheless, up to our knowledge, the parabolic coupled systems of convection-diffusion problems in 2D has not been considered before. In this context, the suitable choice of the numerical time integration is the key for obtaining an efficient numerical algorithm. It is well known that the use of explicit methods is not suitable due

2

to the strong stiffness of the differential systems involved. On the other hand, classical implicit schemes are not optimal due to the computational cost involved in the advance in time, because the resolution of large and complicated linear systems must be faced. In [7,8], an alternating direction method was successfully studied and implemented for time dependent convection-diffusion problems. In such case, only tridiagonal linear systems must be solved to advance in time, resulting that the implicit method was unconditionally convergent and it has a very low computational cost per time step, of the same computational complexity of any explicit method. If the same technique were adapted to the systems considered in this paper, the computational cost per time step is not optimal, specially in the case of considering many equations in the system, because banded linear systems (with a bandwidth which depends on the number of components) should be solved. To avoid this drawback, we consider here a multi-splitting technique, both in directions and in components, in order to get that simple sets of tridiagonal linear systems must be solved to advance in time. In this way, we preserve the main feature of the algorithm proposed in [7] for scalar convection-diffusion problems.

The paper is organized as follows. In section 2, we describe the asymptotic behavior of the exact solution of the continuous problem, giving appropriate bounds for its derivatives which will be used later on to obtain the uniform convergence of the numerical method. In Section 3, we define the spatial discretization on a piecewise uniform mesh of Shishkin type and we prove that the scheme is an almost first order uniformly convergent method. In section 4, we define the time discretization, based on the fractional implicit Euler method (see [4]) and a splitting by components and we prove that it is first order uniformly convergent. As well, we provide a simple technique to elude the order reduction related with the standard choice for the evaluations of the boundary data. In Section 5, we show the numerical results obtained for several test problems, which corroborate in practice the efficiency and the order of uniform convergence of the numerical algorithm. Finally, in Section 6 some concluding remarks are given.

Henceforth, we denote by $\|\mathbf{f}\|_D = \max\{\|f_1\|_D, \|f_2\|_D\}$, where $\|\cdot\|_D$ is the maximum norm on the domain D, by $|\mathbf{v}| = (|v_1|, |v_2|)^T$, $\mathbf{v} \geq \mathbf{w}$ (analogously $\mathbf{v} \leq \mathbf{w}$) means $v_i \geq w_i$ for all i. Finally, $\mathbf{C} = (C, C)^T$, where C is a generic positive constant which is independent of the diffusion parameter ε and the discretization parameters N and M.

2 Asymptotic behavior of the exact solution

In this section we give appropriate estimates for the derivatives of the solution $\mathbf{u}$ of problem (1); from them, we deduce the existence of regular boundary

3

layer of width $\mathcal{O}(\varepsilon)$ at the outflow boundary defined by $\Gamma_1 \cup \Gamma_2$, where $\Gamma_1 = \{(1,y),\ 0 \le y \le 1\}$, $\Gamma_2 = \{(x,1),\ 0 \le x \le 1\}$.

We introduce the scalar uncoupled differential operators

$$\mathcal{L}_{k,\varepsilon}v(\mathbf{x},t) \equiv v_t(\mathbf{x},t) - \varepsilon(v_{xx}(\mathbf{x},t) + v_{yy}(\mathbf{x},t)) + b_{x,kk}v_x(\mathbf{x},t) + b_{y,kk}v_y(\mathbf{x},t) + a_{kk}v(\mathbf{x},t),$$

for $k = 1, 2$, which satisfy a maximum principle (see [17]). Following [19], the next uniform boundedness result can be proved.

Lemma 1. *Let* $w \in C(\bar{Q}) \cap C^2(Q)$ *be such that* $\mathcal{L}_{k,\varepsilon}w = \psi$ *on* Q, $k = 1, 2$, $w = g$ *on* $\partial\Omega \times [0,T]$ *and* $w(\mathbf{x},0) = \varphi$ *on* Ω. *Then, it holds*

$$\|w\|_{\bar{Q}} \le \frac{1}{\beta}\|\psi\|_{\bar{Q}} + \|g\|_{\partial\Omega \times [0,T]} + \|\varphi\|_{\bar\Omega}. \tag{3}$$

Following a similar reasoning to the used one in [5], the following inverse positivity property is deduced for problem (1).

Lemma 2. *Let* $\mathbf{v} \in (C(\bar{Q}) \cap C^2(Q))^\ell$ *be such that* $\mathcal{L}_\varepsilon \mathbf{v} \ge \mathbf{0}$ *on* Q *and* $\mathbf{v} \ge \mathbf{0}$ *on* $\partial\Omega \times [0,T] \cup \Omega \times \{0\}$. *Then,* $\mathbf{v} \ge \mathbf{0}$ *on* $\bar{Q}$.

Using this result joint to the barrier function technique, it can be proved that

$$\|\mathbf{u}\|_{\bar{Q}} \le \frac{1}{\beta}\|\mathbf{f}\|_{\bar{Q}} + \|\mathbf{g}\|_{\partial\Omega \times [0,T]} + \|\boldsymbol{\varphi}\|_{\bar\Omega}. \tag{4}$$

Now, using the idea of extended domains (see [7] for more details), we decompose the solution of (1) as $\mathbf{u} = \mathbf{v} + \mathbf{w}_1 + \mathbf{w}_2 + \mathbf{z}_1$, where $\mathbf{v}$ is the regular component, $\mathbf{w}_i, i = 1, 2$ are the boundary layer functions and $\mathbf{z}_1$ is the corner layer function associated with the corner $(1,1)$.

The regular component can be described as the restriction on $\bar{Q}$ of the solution of

$$
\begin{cases}
\dfrac{\partial \mathbf{v}^*}{\partial t}(\mathbf{x},t) - \varepsilon\Delta\mathbf{v}^* + \mathcal{B}_x^*(\mathbf{x})\dfrac{\partial}{\partial x}\mathbf{v}^* + \mathcal{B}_y^*(\mathbf{x})\dfrac{\partial}{\partial y}\mathbf{v}^* + \mathcal{A}^*(\mathbf{x},t)\mathbf{v}^* = \\
\qquad\qquad\qquad\qquad\qquad \mathbf{f}^*(\mathbf{x},t),\ (\mathbf{x},t) \in Q^* \equiv \Omega^* \times (0,T], \\
\mathbf{v}^*(\mathbf{x},t) = \mathbf{0},\ (\mathbf{x},t) \in \partial\Omega^*, \times[0,T],\ \mathbf{v}^*(\mathbf{x},0) = \boldsymbol{\varphi}^*(\mathbf{x}),\ \mathbf{x} \in \Omega^*,
\end{cases}
$$

where Ω^* is an extension of $\bar\Omega$ with smooth boundary and $B_x^*, B_y^*, A^*, \mathbf{f}^*, \boldsymbol{\varphi}^*$ are suitable smooth extensions (up to Ω^*) of $B_x, B_y, A, \mathbf{f}, \boldsymbol{\varphi}$ respectively. On

4

the other hand, $\mathbf{w}_1$ (similarly $\mathbf{w}_2$) is the restriction on $\bar{Q}$ of the solution of

$$
\begin{cases}
\dfrac{\partial \mathbf{w}_1^{**}}{\partial t}(\mathbf{x},t) - \mathcal{D}\Delta \mathbf{w}_1^{**} + \mathcal{B}_x^*(\mathbf{x})\dfrac{\partial}{\partial x}\mathbf{w}_1^{**} + \mathcal{B}_y^*(\mathbf{x})\dfrac{\partial}{\partial y}\mathbf{w}_1^{**} + \mathcal{A}^*(\mathbf{x},t)\mathbf{w}^{**} = \mathbf{0} \\
\qquad\qquad\qquad\qquad\qquad\qquad (\mathbf{x},t) \in Q^{**} \equiv \Omega^{**} \times (0,T], \\
\mathbf{w}_1^{**}(\mathbf{x},t) = -\mathbf{v}^*(\mathbf{x},t), \ (\mathbf{x},t) \in \partial\Omega_1^{**}, \times [0,T], \\
\mathbf{w}_1^{**}(\mathbf{x},t) = \mathbf{0}, \ (\mathbf{x},t) \in \partial\Omega_2^{**}, \times [0,T], \\
\mathbf{w}_1^{**}(\mathbf{x},0) = \mathbf{0}, \ \mathbf{x} \in \Omega^{**},
\end{cases}
$$

where $\Omega^{**} \subset \Omega^*$ is a small extension of Ω, only around the corner $(1,1)$, whose boundary $\partial\Omega_1^{**}$ is smooth near it and it contains the segment $\{(1,y)|0 \le y \le 1+\delta\}$, for a sufficiently small $\delta > 0$; we denote $\partial\Omega_2^{**} = \partial\Omega^* \backslash \partial\Omega_1^{**}$. Finally, the corner layer function is the solution of

$$
\begin{cases}
\dfrac{\partial \mathbf{z}_1}{\partial t}(\mathbf{x},t) - \mathcal{D}\Delta\mathbf{z}_1 + \mathcal{B}_x(\mathbf{x})\dfrac{\partial}{\partial x}\mathbf{z}_1 + \mathcal{B}_y(\mathbf{x})\dfrac{\partial}{\partial y}\mathbf{z}_1 + \mathcal{A}(\mathbf{x},t)\mathbf{z}_1 = \mathbf{0}, \ (\mathbf{x},t) \in Q, \\
\mathbf{z}_1(\mathbf{x},t) = \mathbf{u}(\mathbf{x},t) - (\mathbf{v}(\mathbf{x},t) + \mathbf{w}_1(\mathbf{x},t) + \mathbf{w}_2(\mathbf{x},t)), \ (\mathbf{x},t) \in \partial\Omega \times [0,T], \\
\mathbf{z}_1(\mathbf{x},0) = \mathbf{0}, \ \mathbf{x} \in \Omega.
\end{cases}
$$

Then, following a similar process to the one which was used in [7], we obtain the following estimates for the derivatives of these components:

$$
\left| \frac{\partial^{k+k_0}}{\partial x^{k_1}\partial y^{k_2}\partial t^{k_0}}\mathbf{v}(\mathbf{x},t) \right| \le \mathbf{C}, \quad (\mathbf{x},t) \in \bar{Q}, \tag{5}
$$

$$
\left| \frac{\partial^{k+k_0}}{\partial x^{k_1}\partial y^{k_2}\partial t^{k_0}}\mathbf{w}_1(\mathbf{x},t) \right| \le \mathbf{C}\varepsilon^{-k} e^{-\frac{\beta(1-x)}{\varepsilon}}, \quad (\mathbf{x},t) \in \bar{Q}, \tag{6}
$$

$$
\left| \frac{\partial^{k+k_0}}{\partial x^{k_1}\partial y^{k_2}\partial t^{k_0}}\mathbf{w}_2(\mathbf{x},t) \right| \le \mathbf{C}\varepsilon^{-k_2} e^{-\frac{\beta(1-y)}{\varepsilon}}, \quad (\mathbf{x},t) \in \bar{Q}, \tag{7}
$$

$$
\left| \frac{\partial^{k+k_0}}{\partial x^{k_1}\partial y^{k_2}\partial t^{k_0}}\mathbf{z}_1(\mathbf{x},t) \right| \le \mathbf{C}\varepsilon^{-k} \min\{e^{-\frac{\beta(1-x)}{\varepsilon}}, e^{-\frac{\beta(1-y)}{\varepsilon}}\}, \quad (\mathbf{x},t) \in \bar{Q}, \tag{8}
$$

with $0 \le k + 2k_0 \le 4$ and $k = k_1 + k_2$.

3 The spatial discretization

In this section we propose a spatial semidiscretization of problem (1). To do that, we use the classical upwind scheme defined on a piecewise uniform rectangular mesh $\overline{\Omega}^N = \overline{I}_x^N \times \overline{I}_y^N$, being $\overline{I}_x^N, \overline{I}_y^N$ 1D meshes of Shishkin type. From the results of the previous section we know that the exact solution of

5

the continuous problem has a regular boundary layer at the outflow boundary $\Gamma_1 \cup \Gamma_2$; therefore, for the variable x (and similarly for the variable y) the grid points of $\overline{I}_x^N \equiv \{0 = x_0 < x_1 < \ldots < x_N = 1\}$ are defined as follows (see [3]). Let N be a positive even number and define the transition parameter

$$\sigma = \min\{1/2, \sigma_0 \varepsilon \ln N\}, \qquad (9)$$

with σ_0 a constant to be fixed later. Then, the grid points are given by

$$x_i = \begin{cases} iH, & i = 0, \ldots, N/2, \\ x_{N/2} + (i - N/2)h, & i = N/2 + 1, \ldots, N, \end{cases}$$

where $h = 2\sigma/N$, $H = 2(1-\sigma)/N$. We denote by $h_{x,i} = x_i - x_{i-1}$, $i = 1, \ldots, N$, and $\overline{h}_{x,i} = (h_{x,i} + h_{x,i+1})/2$, $i = 1, \ldots, N-1$.

Let us denote by Ω^N the subgrid of $\overline{\Omega}^N$ composed only by the interior points of it, i.e., by $\overline{\Omega}^N \cap \Omega$, $\partial\Omega^N \equiv \overline{\Omega}^N \backslash \Omega^N$, by $[\mathbf{v}]_{\Omega^N}$ (analogously $[v]_{\Omega^N}$ for scalar functions) the restriction operators, applied to vector functions defined in Ω, to the mesh Ω^N, and by $[\mathbf{v}]_{\partial\Omega^N}$ (analogously $[v]_{\partial\Omega^N}$ for scalar functions) the restriction operators, applied to vector functions defined on $\partial\Omega$, to the mesh $\partial\Omega^N$. For all $(x_i, y_j) \in \Omega^N$, we introduce the semidiscretization $\mathbf{U}^N(t) \equiv \mathbf{U}_{ij}^N(t)$, $i, j = 1, \ldots N - 1$, with $\mathbf{U}_{ij}^N(t) \approx \mathbf{u}(x_i, y_j, t)$, as the solution of the following Initial Value Problem

$$\begin{cases} \dfrac{d\mathbf{U}^N}{dt}(t) + \mathcal{L}_\varepsilon^N(t)\overline{\mathbf{U}}^N(t) = [\mathbf{u}(\mathbf{x}, t)]_{\Omega^N}, & \text{in } \Omega^N \times [0, T], \\ \overline{\mathbf{U}}^N(t) = [\mathbf{g}(\mathbf{x}, t)]_{\partial\Omega^N}, & \text{in } \partial\Omega^N \times [0, T], \\ \mathbf{U}^N(0) = [\varphi(\mathbf{x})]_{\Omega^N} \end{cases} \qquad (10)$$

where $\overline{\mathbf{U}}^N(t)$ is the natural extension to $\overline{\Omega}^N \times [0, T]$ of the semidiscrete functions $\mathbf{U}^N(t)$, defined on $\Omega^N \times [0, T]$, by adding the corresponding boundary data. As well, $\mathcal{L}_\varepsilon^N(t)$ is the discretization of the operator $\mathcal{L}_{\mathbf{x},\varepsilon}(t)$ using the upwind scheme. i.e.

$$(\mathcal{L}_\varepsilon^N(t)\overline{\mathbf{U}}^N)_{ij,k} = c_{ij,l,k}U_{i-1j,k}^N + c_{ij,r,k}U_{i+1j,k}^N + c_{ij,d,k}U_{ij-1,k}^N +$$
$$c_{ij,u,k}U_{ij+1,k}^N + c_{ij,c,k}U_{ij,k}^N + a_{k1}(t)U_{ij,1}^N + a_{k2}(t)U_{ij,2}^N, \ \ k = 1, 2, \qquad (11)$$

with

$$c_{ij,l,k} = \frac{-\varepsilon}{h_{x,i}\overline{h}_{x,i}} - \frac{b_{x,kk}(x_i, y_j)}{h_{x,i}}, c_{ij,r,k} = \frac{-\varepsilon}{h_{x,i+1}\overline{h}_{x,i}},$$
$$c_{ij,d,k} = \frac{-\varepsilon}{h_{y,j}\overline{h}_{y,j}} - \frac{b_{y,kk}(x_i, y_j)}{h_{y,j}}, c_{ij,u,k} = \frac{-\varepsilon}{h_{y,j+1}\overline{h}_{y,j}}, \qquad (12)$$
$$c_{ij,c,k} = -(c_{ij,l,k} + c_{ij,r,k} + c_{ij,d,k} + c_{ij,u,k}),$$

6

where we denote $a_{kr}(t) = a_{kr}(x_i, y_j, t)$, $k, r = 1, 2$ for $i, j = 1, \ldots N - 1$.

The uniform well-posedness of (10) is a consequence of the following semidiscrete maximum principle (see [6]).

Theorem 1. *Under the assumption $[\mathbf{f}(\mathbf{x}, t)]_{\Omega^N}, \leq \mathbf{0}$, it holds that $\overline{\mathbf{U}}'(t)$ reaches its maximum componentwise value at the boundary $\partial \Omega^N \times [0, T] \cup \Omega^N \times \{0\}$.*

The proof of this result is similar to the proof of the semidiscrete maximum principle stated in [5]. From Theorem 1, the next result follows.

Theorem 2. *If $[\mathbf{f}(\mathbf{x}, t)]_{\Omega^N} \geq \mathbf{0}$, $[\mathbf{g}(\mathbf{x}, t)]_{\partial \Omega^N} \geq \mathbf{0}$ and $[\varphi(\mathbf{x})]_{\Omega^N} \geq \mathbf{0}$, then $\overline{\mathbf{U}}^N(t) \geq \mathbf{0}$.*

Using now a well known barrier-function technique, see [3,19] for instance, the following result can be proved.

Theorem 3. *(Uniform stability for (10)). The unique solution of problem (10) satisfies the uniform bound*

$$\|\overline{\mathbf{U}}^N(t)\|_{\overline{\Omega}^N \times [0,T]} \leq$$
$$\max\{\|[\varphi(\mathbf{x})]_{\Omega^N}\|_{\Omega^N}, \|[\mathbf{g}(\mathbf{x}, t)]_{\partial \Omega^N}\|_{\partial \Omega^N \times [0,T]}, \frac{1}{\beta}\|[\mathbf{f}(\mathbf{x}, t)]_{\Omega^N}\|_{\Omega^N \times [0,T]}\}.$$

The last result in this section proves the uniform convergence of the spatial discretization.

Theorem 4. *Under the previous smoothness assumptions for $\mathbf{u}$, the error associated with the spatial discretization on the Shishkin mesh satisfies*

$$\|\overline{\mathbf{U}}^N(t) - [\mathbf{u}(\mathbf{x}, t)]_{\Omega^N}\|_{\overline{\Omega}^N} \leq C N^{-1} \ln N, \ t \in [0, T], \tag{13}$$

where C is independent of ε and N, and therefore the spatial discretization is an almost first order uniformly convergent scheme.

Proof. To analyze the uniform convergence of the spatial discretization, we decompose the semidiscrete solution in the form

$$\overline{\mathbf{U}}^N(t) = \overline{\mathbf{V}}^N(t) + \sum_{i=1}^{2} \overline{\mathbf{W}}_i^N(t) + \overline{\mathbf{Z}}_1^N(t), \tag{14}$$

where these grid functions are the solution of the semidiscrete problems

$$\begin{cases} \dfrac{d\overline{\mathbf{V}}^N}{dt}(t) + \mathcal{L}_\varepsilon^N(t)\overline{\mathbf{V}}^N(t) = [\mathcal{L}_\varepsilon(t)\mathbf{v}]_{\Omega^N}, & \text{in } \Omega^N \times [0, T], \\ \overline{\mathbf{V}}^N(t) = [\mathbf{v}(\mathbf{x}, t)]_{\partial \Omega^N}, & \text{in } \partial \Omega^N \times [0, T], \\ \mathbf{V}^N(0) = [\mathbf{v}(\mathbf{x}, 0)]_{\Omega^N}, \end{cases}$$

7

$$\begin{cases} \dfrac{d\mathbf{W}_i^N}{dt}(t) + \mathcal{L}_\varepsilon^N(t)\overline{\mathbf{W}}_i^N(t) = [\mathbf{0}]_{\Omega^N}, \text{ in } \Omega^N \times [0,T], \\ \overline{\mathbf{W}}_i^N(t) = [\mathbf{w}_i(\mathbf{x},t)]_{\partial\Omega^N}, \text{ in } \partial\Omega^N \times [0,T], \\ \mathbf{W}_i^N(0) = [\mathbf{w}_i(\mathbf{x},0)]_{\Omega^N}, \end{cases}$$

for $i = 1, 2$ and

$$\begin{cases} \dfrac{d\mathbf{Z}_1^N}{dt}(t) + \mathcal{L}_\varepsilon^N(t)\overline{\mathbf{Z}}_1^N(t) = [\mathbf{0}]_{\Omega^N}, \text{ in } \Omega^N \times [0,T], \\ \overline{\mathbf{Z}}_1^N(t) = [\mathbf{z}_1(\mathbf{x},t)]_{\partial\Omega^N}, \text{ in } \partial\Omega^N \times [0,T], \\ \mathbf{Z}_1^N(0) = [\mathbf{z}_1(\mathbf{x},0)]_{\Omega^N}. \end{cases}$$

On the grid Ω^N, for any $t \in (0,T]$, the vector of truncation errors $\tau^N(t)(\mathbf{u}) = (\tau_1^N(t), \tau_2^N(t))^T$, is given by

$$\tau^N(t)(\mathbf{u}) \equiv [(\frac{\partial}{\partial t} + \mathcal{L}_{\mathbf{x},\varepsilon}(t))\mathbf{u}(\mathbf{x},t)]_{\Omega^N} - (\frac{d}{dt}[\mathbf{u}(\mathbf{x},t)]_{\Omega^N} + \mathcal{L}_\varepsilon^N(t)[\mathbf{u}(\mathbf{x},t)]_{\overline{\Omega}^N}).$$

For the regular component, at the grid points $(x_i, y_j), i, j = 1, \ldots, N-1$, the truncation error satisfies

$$|\tau_{ij}^N(t)(\mathbf{v})| \leq |\mathcal{D}\left(\Delta\mathbf{v}(x_i,y_j,t) - \left(\delta^2 + \delta_y^2\right)\mathbf{v}(x_i,y_j,t)\right)| \\ +\mathbf{C}|\frac{\partial}{\partial x}\mathbf{v}(x_i,y_j,t) - D_x^-\mathbf{v}(x_i,y_j,t)| + \mathbf{C}|\frac{\partial}{\partial y}\mathbf{v}(x_i,y_j,t) - D_y^-\mathbf{v}(x_i,y_j,t)|,$$

where δ_x^2 and δ_y^2 are the discretization on a nonuniform mesh of the second derivatives respect to x and y and D_x^- and D_y^- are the backward discretization on a nonuniform mesh of the first order derivatives respect to x and y.

We analyze the first component of local error in detail; the same reasoning applies directly to the second component. From Taylor expansion, it easily follows that

$$|\tau_{ij,1}^N(t)(\mathbf{v})| \leq C\left(\varepsilon\int_{x_{i-1}}^{x_i}(|\frac{\partial^3 v_1}{\partial x^3}(s)| + |\frac{\partial^3 v_1}{\partial y^3}(s)|)ds + \int_{x_{i-1}}^{x_i}(|\frac{\partial^2 v_1}{\partial x^2}(s)| + |\frac{\partial^2 v_1}{\partial y^2}(s)|)ds\right).$$

Then, from the estimates (5) it holds

$$|\tau^N(t)(\mathbf{v})| \leq \mathbf{C}N^{-1}.$$

Then, the semidiscrete comparison principle allows to establish that

$$|(\mathbf{V}^N - \mathbf{v})(x_i,y_j,t)| \leq \mathbf{C}N^{-1}. \tag{15}$$

Next, we analyze the error associated with the boundary layer functions $\mathbf{w}_i, i =$

8

1, 2. We give some details only for $\mathbf{w}_1$, and in a similar way the other one can be obtained. The analysis depends on the location of grid point x_i.

First, we assume that $0 < x_i \leq 1 - \sigma$. We define the barrier function $\boldsymbol{\Psi} = (\Psi, \Psi)^T$ with $\Psi = S_{x,i}(\beta)$, where

$$S_{x,i}(\beta) = \begin{cases} \prod_{s=i+1}^{N} \left(1 + h_{x,i}\beta/\varepsilon \right)^{-1}, \, i \neq N, \\ 1, \, i = N, \end{cases} .$$

Then, using the barrier function $\boldsymbol{\Psi}$, and taking into account the estimates (6) and using that $S_{x,i}(\beta) \leq CN^{-1}$, for $0 < x_i \leq 1 - \sigma$, we have

$$|(\mathbf{W}_1^N - \mathbf{w}_1)(x_i, y_j, t)| \leq \mathbf{C} \, N^{-1}. \tag{16}$$

For the grid points $(x_i, y_j) \in (1 - \sigma, 1) \times (0, 1)$, using the bounds (6), we find that the local error satisfies

$$|\tau_{ij}^N(t)(\mathbf{w}_1)| \leq \mathbf{C} \, \varepsilon^{-1} h$$

and taking into account that $h \leq C \, \varepsilon N^{-1} \ln N$, we obtain

$$|(\mathbf{W}_1^N - \mathbf{w}_1)(x_i, y_j, t)| \leq \mathbf{C}N^{-1} \ln N. \tag{17}$$

Finally, we analyze the error associated with the corner layer function $\mathbf{z}_1$. If $0 < x_i \leq 1 - \sigma, 0 < y_j \leq 1 - \sigma$, or $0 < x_i \leq 1 - \sigma, 1 - \sigma < y_j < 1$ or $1 - \sigma < x_i < 1, 0 < y_j \leq 1 - \sigma$, using that $\mathbf{z}_1$ decays exponentially from $y = 1$ and the definition of the transition point σ, proceeding in the same way as for the analysis of $\mathbf{w}_1$, it follows

$$|(\mathbf{Z}_1^N - \mathbf{z}_1)(x_i, y_j, t)| \leq \mathbf{C}N^{-1}. \tag{18}$$

At last, for the grid points $(x_i, y_j) \in (1 - \sigma, 1) \times (1 - \sigma, 1)$, the error estimates are deduced using a classical truncation error analysis (see [9,19]) and making use that the mesh is fine in both spatial directions; in this case, it holds

$$|(\mathbf{Z}_1^N - \mathbf{z}_1)(x_i, y_j, t)| \leq \mathbf{C}N^{-1} \ln N. \tag{19}$$

From (15)-(19), the required result follows. $\qquad \square$

4 The fully discrete scheme: uniform convergence

The second step to find the fully discrete method, consists in to apply an appropriate time integrator to the semidiscrete problems (10). To simplify the

notations, we introduce the difference operators

$$
\begin{aligned}
\mathcal{L}_{x,1}^N(t)v^N &\equiv -\varepsilon\partial_{xx}v^N + b_{x,11}\partial_x v^N + a_{x,11}(t)v^N, \\
\mathcal{L}_{y,1}^N(t)v^N &\equiv -\varepsilon\partial_{yy}v^N + b_{y,11}\partial_y v^N + a_{y,11}(t)v^N, \\
\mathcal{L}_{x,2}^N(t)v^N &\equiv -\varepsilon\partial_{xx}v^N + b_{x,22}\partial_x v^N + a_{x,22}(t)v^N, \\
\mathcal{L}_{y,2}^N(t)v^N &\equiv -\varepsilon\partial_{yy}v^N + b_{y,22}\partial_y v^N + a_{y,22}(t)v^N,
\end{aligned}
\tag{20}
$$

being ∂_{xx} and ∂_{yy} the classical second order central differences, and ∂_x, ∂_y the forward approximation of first derivatives, on the corresponding one dimensional Shishkin meshes, with $a_{x,kk}(x,y,t) + a_{y,kk}(x,y,t) = a_{kk}(x,y,t), k = 1,2$. We will choose that $a_{z,kk}(x,y,t) \geq 0, \; k = 1,2, z = x,y$. Analogously, we decompose the non diagonal coefficients of the reaction matrix in the form $a_{x,kr}(x,y,t) + a_{y,kr}(x,y,t) = a_{kr}(x,y,t), \; k,r = 1,2, k \neq r$, choosing that $a_{z,kr}(x,y,t) \leq 0, \; k,r = 1,2, k \neq r, z = x,y$, and $\sum_{r=1}^{2} a_{z,kr}(x,y,t) \geq \alpha_z > 0, k = 1,2, z = x,y \; (\alpha_x + \alpha_y = \alpha)$. Notation $a_{z,kr}(t)v^N$ must be understood as follows: $(a_{z,kr}(t)v^N)_{kl} \equiv a_{z,kr}(x_i,y_j,t)v_{kl}^N$; as well, we decompose the right-hand side $\mathbf{f}(\mathbf{x},t) \equiv (f_1,f_2)^T$, in the form $\mathbf{f}_x + \mathbf{f}_y = (f_{x,1},f_{x,2})^T + (f_{y,1},f_{y,2})^T$.

Then, the fully discrete scheme is given by

0) (initialize) $\mathbf{U}^{N,0} = [\boldsymbol{\varphi}]_{\overline{\Omega}^N}$,

$$
\begin{cases}
\text{(first half step)} \\
1)(I + \tau\mathcal{L}_{x,1}^N(t_{m+1}))U_1^{N,m+1/2} = U_1^{N,m} + \tau F_{x,1}^{m+1} - \tau a_{x,12}(t_{m+1})U_2^{N,m}, \quad \text{in } \Omega_x^N, \\
2)(I + \tau\mathcal{L}_{x,2}^N(t_{m+1}))U_2^{N,m+1/2} = U_2^{N,m} + \tau F_{x,2}^{m+1} - \tau a_{x,21}(t_{m+1})U_1^{N,m+1/2}, \quad \text{in } \Omega_x^N, \\
\mathbf{U}_{0,j}^{N,m+1/2} = \mathbf{G}_{0,j}^{N,m+1/2}, \mathbf{U}_{N,j}^{N,m+1/2} = \mathbf{G}_{N,j}^{N,m+1/2}, j = 0,\dots,N, \\
\text{(second half step)} \\
3)(I + \tau\mathcal{L}_{y,2}^N(t_{m+1}))U_2^{N,m+1} = U_2^{N,m+1/2} + \tau F_{y,2}^{m+1} - \tau a_{y,21}(t_{m+1})U_1^{N,m+1/2}, \quad \text{in } \Omega_y^N, \\
4)(I + \tau\mathcal{L}_{y,1}^N(t_{m+1}))U_1^{N,m+1} = U_1^{N,m+1/2} + \tau F_{y,1}^{m+1} - \tau a_{y,12}(t_{m+1})U_2^{N,m+1}, \quad \text{in } \Omega_y^N, \\
\mathbf{U}_{i,0}^{N,m+1} = \mathbf{G}_{i,0}^{N,m+1}, \mathbf{U}_{i,N}^{N,m+1} = \mathbf{G}_{i,N}^{N,m+1}, i = 0,\dots,N, \\
\qquad\qquad m = 0,\dots,M-1,
\end{cases}
\tag{21}
$$

where $\tau \equiv T/M$ is the time step, $t_m = m\tau, m = 0,\dots,M$ are the intermediate times where the semidiscrete solution $\overline{\mathbf{U}}(t_m)$ is approximated as $\mathbf{U}^{N,m}$, $\Omega_x^N \equiv I_x^N \times \overline{I}_y^N, \Omega_y^N \equiv \overline{I}_x^N \times I_y^N$,

$$
F_{z,k}^{m+1} \equiv [f_{z,k}(\mathbf{x},t_{m+1})]_{\Omega_z^N}, k = 1,2, z = x,y, \tag{22}
$$

10

and the discrete boundary data are given by

$$
\begin{aligned}
\mathbf{G}_0^{N,m+1/2} &= \Big((I + \tau \mathcal{L}_{y,1}^N(t_{m+1}))[g_1(0,y,t_{m+1})]_{\bar{I}_y} - \tau[f_{y,1}(0,y,t_{m+1})]_{I_y} + \\
&\quad [\tau a_{y,12}(0,y,t_{m+1})g_2(0,y,t_{m+1})]_{I_y}, \\
&\qquad (I + \tau \mathcal{L}_{y,2}^N(t_{m+1}))[g_2(0,y,t_{m+1})]_{\bar{I}_y} - \tau[f_{y,2}(0,y,t_{m+1})]_{I_y} + \\
&\quad [\tau a_{y,21}(0,y,t_{m+1})g_1(0,y,t_{m+1})]_{I_y} \Big)^T, \\
\mathbf{G}_N^{N,m+1/2} &= \Big((I + \tau \mathcal{L}_{y,1}^N(t_{m+1}))[g_1(1,y,t_{m+1})]_{\bar{I}_y} - \tau[f_{y,1}(1,y,t_{m+1})]_{I_y} + \\
&\quad [\tau a_{y,12}(1,y,t_{m+1})g_2(1,y,t_{m+1})]_{I_y}, \\
&\qquad (I + \tau \mathcal{L}_{y,2}^N(t_{m+1}))[g_2(1,y,t_{m+1})]_{\bar{I}_y} - \tau[f_{y,2}(1,y,t_{m+1})]_{I_y} + \\
&\quad [\tau a_{y,21}(1,y,t_{m+1})g_1(1,y,t_{m+1})]_{I_y} \Big)^T, \\
\mathbf{G}_0^{N,m+1} &= [\mathbf{g}(x,0,t_{m+1})]_{I_x} \text{ and } \mathbf{G}_N^{N,m+1} = [\mathbf{g}(x,1,t_{m+1})]_{I_x}
\end{aligned}
\tag{23}
$$

Note that in the half steps of (21), only tridiagonal linear systems must be solved to obtain $\mathbf{U}^{N,\bullet}$. Therefore, the computational cost of our algorithm is similar to the cost of any one step explicit method; for the same reason, the method has a computational cost considerably smaller than the one of implicit classical schemes.

With respect to the proposed boundary data, we wish remark that our proposal provides solutions that are more accurate than those ones obtained with the simpler and, arguably, more obvious formulation

$$
\begin{aligned}
\mathbf{G}_0^{N,m+1/2} &= [\mathbf{g}(0,y,t_{m+1})]_{\bar{I}_y}, \ \mathbf{G}_N^{N,m+1/2} = [\mathbf{g}(1,y,t_{m+1})]_{\bar{I}_y}, \\
\mathbf{G}_0^{N,m+1} &= [\mathbf{g}(x,0,t_{m+1})]_{I_x} \text{ and } \mathbf{G}_N^{N,m+1} = [\mathbf{g}(x,1,t_{m+1})]_{I_x}.
\end{aligned}
\tag{24}
$$

which provokes a reduction in the order of consistency. This reduction in the order of consistency makes difficult to complete the analysis of uniform convergence of this choice.

Let us study now the approximation properties of our proposal. Firstly, we state an inverse positivity result for our fully discrete scheme, which is the discrete analogue of Theorem 2 of the previous section.

Theorem 5. *If all of the data* $(\mathbf{G}, \mathbf{F}_1, \mathbf{F}_2, [\boldsymbol{\varphi}]_{\Omega^N}$ *in (21), have non-negative components, then the solutions* $\mathbf{U}^{N,m}$ *of (21) have non-negative components.*

The proof of this result uses an induction principle on the fractional steps of (21) which is similar to the used one in [4].

To complete the analysis of the uniform convergence of our algorithm, now we rewrite it in such a way that the fractional implicit Euler method is clearly

11

involved:

(initialize) $\mathbf{U}^{N,0} = [\boldsymbol{\varphi}]_{\overline{\Omega}^N}$,

$$
\begin{cases}
\begin{cases}
(I + \tau L^N_{\varepsilon,k}(t_{m+1}))\mathbf{U}^{N,m+k/4} = \mathbf{U}^{N,m+(k-1)/4} + \tau \mathbf{F}^{m+k/4}, & \text{in } \Omega_j^N, \\
\mathbf{U}^{N,m+k/4} = \mathbf{G}^{N,m+k/4}, \text{in } \partial\Omega_k^N, \\
k = 1,2,3,4,
\end{cases} \\
m = 0,\ldots,M-1,
\end{cases}
\tag{25}
$$

where $\Omega_1^N = \Omega_2^N \equiv \Omega_x^N$, $\Omega_3^N = \Omega_4^N \equiv \Omega_y^N$, and

$$
L^N_{\varepsilon,1}(t_{m+1}) \equiv \begin{pmatrix} \mathcal{L}^N_{x,1}(t_{m+1}) & a_{x,12}(t_{m+1}) \\ 0 & I \end{pmatrix}, \quad L^N_{\varepsilon,2}(t_{m+1}) \equiv \begin{pmatrix} I & 0 \\ a_{x,21}(t_{m+1}) & \mathcal{L}^N_{x,2}(t_{m+1}) \end{pmatrix},
$$

$$
L^N_{\varepsilon,3}(t_{m+1}) \equiv \begin{pmatrix} I & 0 \\ a_{y,21}(t_{m+1}) & \mathcal{L}^N_{y,2}(t_{m+1}) \end{pmatrix}, \quad L^N_{\varepsilon,4}(t_{m+1}) \equiv \begin{pmatrix} \mathcal{L}^N_{y,1}(t_{m+1}) & a_{y,12}(t_{m+1}) \\ 0 & I \end{pmatrix},
$$

$$
\mathbf{F}^{m+1/4} \equiv \begin{pmatrix} F_{x,1}^{m+1} \\ 0 \end{pmatrix}, \mathbf{F}^{m+2/4} \equiv \begin{pmatrix} 0 \\ F_{x,2}^{m+1} \end{pmatrix}, \mathbf{F}^{m+3/4} \equiv \begin{pmatrix} 0 \\ F_{y,2}^{m+1} \end{pmatrix}, \mathbf{F}^{m+1} \equiv \begin{pmatrix} F_{y,1}^{m+1} \\ 0 \end{pmatrix},
$$

$\mathbf{G}^{N,m+1/2}$, $\mathbf{G}^{N,m+1}$ are given in (23), $\mathbf{G}^{N,m+1/4} \equiv (\mathbf{G}_1^{N,m+1/2}, [U_2^{N,m}]_{\partial\Omega_1^N})^T$ and $\mathbf{G}^{N,m+3/4} \equiv ([U_1^{N,m+1/2}]_{\partial\Omega_3^N}, \mathbf{G}_2^{N,m+1})^T$, being $\partial\Omega_1^N = \partial\Omega_2^N \equiv \{0,1\} \times \bar{I}_y$ and $\partial\Omega_3^N = \partial\Omega_4^N \equiv \bar{I}_x \times \{0,1\}$.

Using this rewriting, combined with the previous inverse positivity result, we are ready to state the uniform stability and the uniform consistency of our time integration process.

Corollary 1. *(Contractivity of the time integrator).* If $\mathbf{G} = 0, \mathbf{F}_1 = 0$ and $\mathbf{F}_2 = 0$, it holds

$$
\|\mathbf{U}^{N,m+1}\|_{\Omega_N} \leq \|\mathbf{U}^{N,m}\|_{\Omega_N}, \; m = 0,1,\ldots,M-1.
\tag{26}
$$

The proof of this result requires the use of the barrier function technique in a similar way as in [4].

To analyze the uniform consistency, we introduce the local errors in time, as usual:

$$
\mathbf{e}^{N,m+1} \equiv \overline{\mathbf{U}}^N(t_{m+1}) - \widehat{\mathbf{U}}^{N,m+1},
$$

where $\widehat{\mathbf{U}}^{N,m+1}$ is the result which is obtained with the step m of scheme (25) if we change $\mathbf{U}^{N,m}$ by $\overline{\mathbf{U}}^N(t_m)$.

Theorem 6. *(Uniform consistency of the time integrator). Assuming that* $\mathbf{u} \in C^{4,2}(\overline{Q})$, *it holds*

$$\|\mathbf{e}^{N,m+1}\|_{\overline{\Omega}_N} \le CM^{-2}, \quad \forall \, \tau \in (0, \tau_0] \;\; and \;\; \forall \, m = 0, 1, \ldots, M - 1. \quad (27)$$

Proof. We make use of the following Taylor expansion for $\mathbf{U}_{ij}^N(t_m)$, $i, j = 1 \ldots N - 1$

$$\mathbf{U}_{ij}^N(t_m) = \mathbf{U}_{ij}^N(t_{m+1}) - \tau \frac{d\mathbf{U}_{ij}^N}{dt}(t_{m+1}) + \mathcal{O}(\tau^2).$$

As $\mathbf{U}_N$ is the solution of (10), we can substitute the term $\frac{d\mathbf{U}_{ij}^N}{dt}(t_{m+1})$ by

$$\sum_{k=1}^4 (L_{\varepsilon,k}^N(t_{m+1})\overline{\mathbf{U}}^N(t_{m+1}) - \mathbf{F}^{m+k/4})_{ij}$$

to deduce

$$\prod_{k=1}^4 (I + \tau L_{\varepsilon,k}^N(t_{m+1}))\overline{\mathbf{U}}^N(t_{m+1}) = \mathbf{U}^N(t_m) + \tau \sum_{k=1}^4 \prod_{l=1}^{k-1}(I + L_{\varepsilon,l}^N(t_{m+1}))\mathbf{F}^{m+k/4} + \mathcal{O}(\tau^2),$$

in Ω^N. On the other hand, for the values of $\overline{\mathbf{U}}^N(t_{m+1})$ at the boundaries Ω_j^N, it is obvious that $\overline{\mathbf{U}}^N(t_{m+1}) = \mathbf{G}^{m+1}$ in $\partial\Omega_4^N$; as well, the remaining boundary data given by (23) have been chosen in such a way that

$$\prod_{k=4-l+1}^4 (I + \tau L_{\varepsilon,k}^N(t_{m+1}))\overline{\mathbf{U}}^N(t_{m+1}) = \mathbf{G}^{m+1-l/4} \;\; \text{in } \partial\Omega_{4-l}^N; \; l = 1, 2, 3.$$

Therefore, $\overline{\mathbf{U}}^N(t_{m+1})$ can be described as the solution of

$$\overline{\mathbf{U}}^{N,m} = \mathbf{U}^N(t_m) + \mathcal{O}(\tau^2),$$

$$\begin{cases} (I + \tau L_{\varepsilon,k}^N(t_{m+1}))\overline{\mathbf{U}}^{N,m+k/4} = \overline{\mathbf{U}}^{N,m+(k-1)/4} + \tau\mathbf{F}^{m+k/4}, \;\; \text{in } \;\; \Omega_k^N, \\ \overline{\mathbf{U}}^{N,m+k/4} = \mathbf{G}^{N,m+k/4}, \text{in } \partial\Omega_k^N, \\ k = 1, 2, 3, 4. \end{cases} \quad (28)$$

Subtracting this scheme and the corresponding one which defines $\widehat{\mathbf{U}}_N^{m+1}$, it is immediate that $\mathbf{e}^{N,m+1}$ is the solution of a problem of the form

$$\mathbf{e}^{N,m} = \mathcal{O}(\tau^2),$$

$$\begin{cases} (I + \tau L_{\varepsilon,k}^N(t_{m+1}))\mathbf{e}^{N,m+k/4} = \mathbf{e}^{N,m+(k-1)/4}, \;\; \text{in } \;\; \Omega_k^N, \\ \mathbf{e}^{N,m+k/4} = \mathbf{0}, \text{in } \partial\Omega_k^N, \\ k = 1, 2, 3, 4, \end{cases} \quad (29)$$

13

Using now (26), the required result follows. $\qquad\qquad\qquad\qquad\square$

A classical combination of (27) and (26), allows to establish that the time integration process is uniformly convergent of first order (see [4,5] for more details), i.e.

$$\|\overline{\mathbf{U}}^N(t_m) - \mathbf{U}^{N,m}\|_{\overline{\Omega}^N} \le \sum_{s=1}^m \|\mathbf{e}^{N,s}\|_{\overline{\Omega}^N} \le CM^{-1} \qquad (30)$$

Joining now (13) and (30), the main uniform convergence result of this paper is deduced (see [4] for more details).

Theorem 7. *(Uniform convergence) Assuming that* $\iota \in C^{4,}(\overline{Q})$, *the global error associated with the numerical method defined by (21), (23) satisfies*

$$\max_{0\le m\le M} \|\mathbf{U}^{N,m} - [\mathbf{u}(\mathbf{x},t_m)]_{\overline{\Omega}^N}\|_{\overline{\Omega}^N} \le C\left(N^{-}\ln N + M^{-1}\right), \qquad (31)$$

where the constant C *is independent of the diffusion parameter* ε *and the discretization parameters* N *and* M.

5 Numerical results

In this section we show the numerical results obtained with the algorithm proposed here to solve successfully some problems of type (1).

Example 1. The matrices of the first example are given by

$$\mathcal{A} = \begin{pmatrix} 4 + (x-y)t^2 & -(x+y^2)(1-e^{-t}) \\ -\sin(xy)t^2 & 1 - e^{-t(x+y)} \end{pmatrix}, \qquad (32)$$

$$\mathcal{B}_x = \mathrm{diag}(3 - xy, 2 + e^{-xy}), \ \mathcal{B}_y = \mathrm{diag}(3 - x^2 - y^2, 3 - x - y),$$

and the rest of data are defined by

$$\mathbf{f}(\mathbf{x},t) = (\sin(x-y)(1-e^{-t}), -10(x^2+y^2)t^2))^T, \mathbf{g} = ((x+y)t^2, xy(e^t-1))^T, \varphi = \mathbf{0}.$$

Figure 1 displays the numerical solution at $T = 1$ for $\varepsilon = 10^{-4}$. From it, we clearly see the regular boundary layers at the outflow of the spatial domain.

As the exact solution is unknown we cannot calculate exactly the errors; instead of it, we estimate them by using a variant of the double-mesh principle (see [4]). These estimated maximum errors are given by

$$\mathbf{d}_\varepsilon^{N,M} = \max_{0\le m\le M} \max_{0\le i,j\le N} |\mathbf{U}_{ij}^{N,m} - \widehat{\mathbf{U}}_{2i\,2j}^{2N,2m}|,$$

14

Fig. 1. Components u_1 (left) and u_2 (right) at $T = 1$ for $\varepsilon = 10^{-4}$ with $N = 32, M = 32$
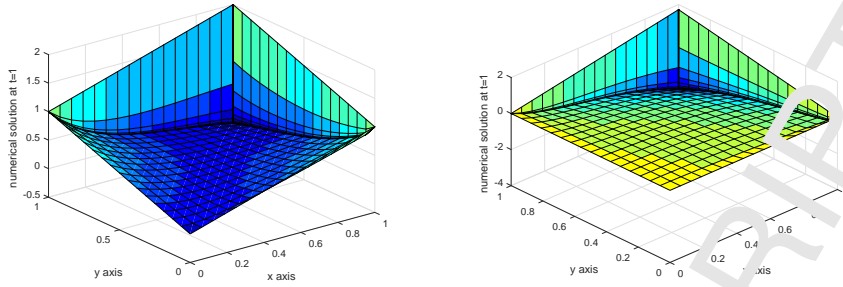
where $\{\widehat{\mathbf{U}}_{ij}^{2N,m}\}$ is the numerical solution on a finer mesh $\{(\hat{x}_i, \hat{y}_j, \hat{t}_m)\}$, which has the mesh points of the coarse mesh and their midpoints. From the maximum two-mesh differences $\mathbf{d}_\varepsilon^{N,M}$, we obtain the ε-uniform two-mesh differences by

$$\mathbf{d}^{N,M} = \max_\varepsilon \mathbf{d}_\varepsilon^{N,M}.$$

From $\mathbf{d}_\varepsilon^{N,M}$, the numerical orders of convergence are calculated by

$$\mathbf{q}_\varepsilon^{N,M} = \log\left(\mathbf{d}_\varepsilon^{N,M}/\mathbf{d}_\varepsilon^{2N,2M}\right)/\log 2,$$

and from $\mathbf{q}^{N,M}$, the numerical uniform orders of uniform convergence are calculated by

$$\mathbf{q}^{N,M} = \log\left(\mathbf{d}^{N,M}/\mathbf{d}^{2N,2M}\right)/\log 2.$$

As the algorithm requires a suitable smooth partition of the reaction matrix, for simplicity, here we have chosen

$$a_{x,kr}(x,y,t) = a_{y,kr}(x,y,t) = a_{kr}(x,y,t)/2, \ k,r = 1,2. \tag{33}$$

Moreover, we have taken (see [3,7])

$$
\begin{aligned}
f_{y,k}(x,y,t) &= f_k(x,0,t) + y(f_k(x,1,t) - f_k(x,0,t)), \\
f_{x,k}(x,y,t) &= f_k(x,y,t) - f_{y,k}(x,y,t), \ k = 1,2,
\end{aligned}
\tag{34}
$$

to decompose the right-hand side of the differential equation.

Tables 1 and 2 show the results for some values of ε for the first and the second components respectively, taking $\sigma_0 = 1.2$ in (9). From them, we clearly deduce the uniform convergence of the algorithm of almost first order according to the theoretical results.

Example 2. In order to show the influence of the chosen boundary data on the errors, we have chosen another example. The matrices of this example are

15

Table 1
Maximum errors and orders of convergence in **Example 1** for u_1

ε	N=16 M=8	N=32 M=16	N=64 M=32	N=128 M=64	N=256 M=128
2^{-6}	1.4137E-1 0.5602	9.5876E-2 0.6339	6.1784E-2 0.6954	3.8154E-2 0.7503	2.2682E-2
2^{-8}	1.3562E-1 0.5997	8.9498E-2 0.6135	5.8496E-2 0.6810	3.6486E-2 0.7415	2.1823E-2
2^{-10}	1.3601E-1 0.6676	8.5626E-2 0.6099	5.6106E-2 0.6690	3.5287E-2 0.7249	2.1350E-2
2^{-12}	1.3610E-1 0.6903	8.4342E-2 0.6133	5.5135E-2 0.6682	3.4697E-2 0.6860	2.1 E-2
...	... ...	... ...	... ...	... ..	...
2^{-22}	1.3613E-1 0.6987	8.3872E-2 0.6144	5.4786E-2 0.6697	3.44 0E- 6704	2.1640E-2
$d_1^{N,M}$ $q_1^{N,M}$	1.4137E-1 0.5602	9.5876E-2 0.6339	6.1784E-2 0.6954	3.8154E-2 7503	2.2682E-2

Table 2
Maximum errors and orders of convergence in **Example 1** for u_2

ε	N=16 M=8	N=32 M=16	N=64 M=32	N=128 M=64	N=256 M=128
2^{-6}	2.7063E-1 0.6218	1.7587E-1 0.8137	1. 005E-1 0. 15	5.3191E-2 0.7936	3.0687E-2
2^{-8}	3.1378E-1 0.6413	2.0118E-1 829	1. 324E-1 0.9228	5.9733E-2 0.9600	3.0707E-2
2^{-10}	3.2690E-1 0.6345	058E-1 0.844	1.1728E-1 0.9273	6.1672E-2 0.9598	3.1708E-2
2^{-12}	3.3040E- 0.63	1328 -1 495	1.1836E-1 0.9278	6.2219E-2 0.9598	3.1988E-2
...	.. 	... ...	... ...	... ...	...
2^{-22}	3.315 E-1 303	2.1422E-1 0.8481	1.1900E-1 0.9309	6.2420E-2 0.9598	3.2092E-2
$d_2^{N,M}$ $q_2^{N,M}$	3159E-1 0. 303	2.1422E-1 0.8481	1.1900E-1 0.9309	6.2420E-2 0.9598	3.2092E-2

given by

$$\mathcal{A} = \begin{pmatrix} 10 & -2^{16}(10x^4(1-x)^4y^4(1-y)^4) \\ -2^{16}(20x^4(1-x)^4y^4(1-y)^4) & 20 \end{pmatrix}, \quad (35)$$

$$\mathcal{B}_x = \mathrm{diag}(1,1), \ \mathcal{B}_y = \mathrm{diag}(1,1),$$
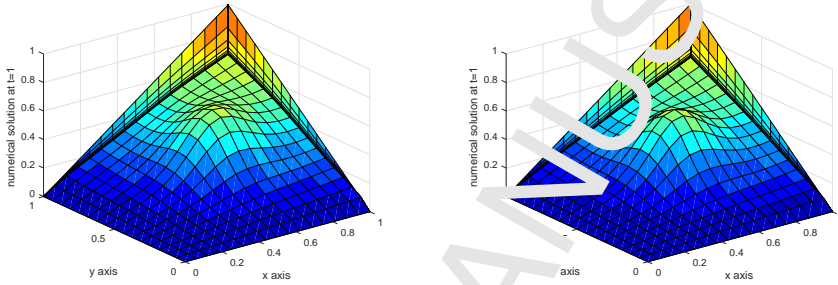
16

and the rest of data are defined by

$$\mathbf{f}(\mathbf{x}, t) = ((1 - e^{-5t})(x + y) + 5xy, (1 - e^{-10t})(x + y) + 10xy)^T,$$

$$\mathbf{g} = (xy(1 - e^{-5t}), xy(1 - e^{-10t}))^T, \varphi = \mathbf{0}.$$

and $T = 1$.

Figure 2 displays the numerical solution at $T = 1$ for $\varepsilon = 10^{-4}$. From it, we clearly see the regular boundary layers at the outflow of the spatial domain.

Fig. 2. Components u_1 (left) and u_2 (right) at $T = 1$ for $\varepsilon = 10^{-4}$ with $N = 32, M = 32$

We estimate the numerical errors and the orders of convergence using the same double mesh principle as in the previous example. We use again the decomposition given in (33) and (34) for the reaction matrix and the right-hand side of the differential equation, respectively. Tables 3, 4 show the results for some values of ε for first and second component respectively. These results correspond to the use of the improved boundary data given in (23). Tables 5, 6 show the results when the standard boundary data (24) are chosen. From them, we see that, in the case of using the standard boundary data, the maximum errors are larger and the orders of convergence are lower for all values of ε.

Example 3. To show that our ideas are easily extended to systems with more components, we consider an example which has three equations. Now the matrices are given by

$$\mathcal{A} = \begin{pmatrix} e^{x+y}(1+t) & -t(x+y) & -tx \\ -(x+y) & (1+t)(3+x+y) & -t\sin(y) \\ -xy^2 & -t(\sin(x)+\sin(y)) & e^t(2+\cos(x+y)) \end{pmatrix},$$

$$\mathcal{B}_x = \mathrm{diag}(1 + xy/2, 5 + x^2 y, 3 - xy), \ \mathcal{B}_y = \mathrm{diag}(e^{x^2 y}, 3 + \sin(x + y), 1 + x + y),$$

$$(36)$$

17

Table 3
Maximum errors and orders of convergence in **Example 2** for u_1 with improved boundary conditions

ε	N=16 M=8	N=32 M=16	N=64 M=32	N=128 M=64	N=256 M=128
2^{-6}	5.4353E-2 0.5682	3.6659E-2 0.6862	2.2783E-2 0.7956	1.3125E-2 0.8796	7.1339E-3
2^{-8}	5.6112E-2 0.5278	3.8920E-2 0.6586	2.4656E-2 0.7497	1.4664E-2 0.8444	8.1668E-3
2^{-10}	5.5969E-2 0.5021	3.9518E-2 0.6446	2.5278E-2 0.7356	1.5181E-2 0.8325	8.2247E-3
2^{-12}	5.5863E-2 0.4943	3.9657E-2 0.6402	2.5444E-2 0.7330	1.5308E-2 0.8285	8.6204E-3
...	... ...	... ...	... ...	... .	...
2^{-22}	5.5821E-2 0.4916	3.9702E-2 0.6387	2.5500E-2 0.7322	1.5350E-2 0.8265	8.6534E-3
$d_1^{N,M}$ $q_1^{N,M}$	5.6112E-2 0.4991	3.9702E-2 0.6387	2.5500E-2 0.7322	1.5350E-2 0.8269	8.6534E-3

Table 4
Maximum errors and orders of convergence in **Example 2** for u_2 with improved boundary conditions

ε	N=16 M=8	N=32 M=16	N=64 M=32	N=128 M=64	N=256 M=128
2^{-6}	7.3169E-2 0.3935	5.5703E-2 0.6377	3.5803E-2 0.7864	2.0759E-2 0.8759	1.1312E-2
2^{-8}	7.3168E-2 0.3935	5.5702E-2 0.6377	3.5803E-2 0.7864	2.0759E-2 0.8759	1.1311E-2
2^{-10}	7.3374E-2 0.3927	5.5890E-2 0.6357	3.6048E-2 0.7845	2.0928E-2 0.8756	1.1406E-2
2^{-12}	7.3226E-2 0.3931	5.5772E-2 0.6361	3.5880E-2 0.7850	2.0823E-2 0.8743	1.1359E-2
...	... .	... ...	... ...	... ...	...
2^{-22}	7.3168E-2 0.3935	5.5702E-2 0.6377	3.5803E-2 0.7864	2.0759E-2 0.8759	1.1311E-2
$d_2^{N,M}$ $q_2^{N,M}$	7.3629E-2 0.3930	5.6072E-2 0.6338	3.6136E-2 0.7880	2.0928E-2 0.8756	1.1406E-2

and the rest of data are defined by

$$\mathbf{f}(x,t) = (10t^2\sin(x+y), -5(1-e^{-t})(x^2+y^2), -4te^t\cos(xy))^T,$$

$$\mathbf{g} = (4(x+y)\sin(t), xyt^2, 3e^{xy}(1-e^t))^T, \varphi = \mathbf{0}.$$

To obtain numerical solutions, we have used the same ideas that in [5] for

18

Table 5
Maximum errors and orders of convergence in **Example 2** for u_1 with standard boundary conditions

| ε	N=16 M=8	N=32 M=16	N=64 M=32	N=128 M=64	N=256 M=128
2^{-6}	5.7604E-2 0.1362	5.2413E-2 0.4040	3.9613E-2 0.6342	2.5523E-2 0.7545	1.5129E-2
2^{-8}	6.0507E-2 0.5278	5.7951E-2 0.6586	4.3880E-2 0.7497	2.7898E-2 0.8444	1.5979E-2
2^{-10}	6.1712E-2 0.0476	5.9708E-2 0.3946	4.5419E-2 0.6510	2.8924E-2 0.8083	1.6517E-2
2^{-12}	6.2029E-2 0.0432	6.0201E-2 0.3920	4.5876E-2 0.6495	2.9246E-2 0.8075	1.6711E-2
...	... ...	... ...	... ...	.. .	...
2^{-22}	6.2137E-2 0.0416	6.0372E-2 0.3910	4.6039E-2 0.6487	2.9367E-2 0.8068	1.6787E-2
$d_1^{N,M}$ $q_1^{N,M}$	6.2137E-2 0.0416	6.0372E-2 0.3910	4.6039E-2 0.6487	2.9367E-2 0.8068	1.6787E-2

Table 6
Maximum errors and orders of convergence in **Example 2** for u_2 with standard boundary conditions

ε	N=16 M=8	N=32 M=16	N=64 M=32	N=128 M=64	N=256 M=128
2^{-6}	7.2865E-2 0.3232	5.8239E-2 0.0492	5.6286E-2 0.4059	4.2482E-2 0.6540	2.6997E-2
2^{-8}	7.4212E-2 0.2096	6.4178E-2 0.0410	6.2380E-2 0.4251	4.6460E-2 0.6765	2.9069E-2
2^{-10}	7.3945E-2 0.1623	6.6076E-2 0.0320	6.4628E-2 0.4232	4.8198E-2 0.6814	3.0055E-2
2^{-12}	7.3796E-2 0.1476	6.6613E-2 0.0287	6.5304E-2 0.4218	4.8749E-2 0.6807	3.0412E-2
...	... ...	... ...	... ...	... ...	...
2^{-22}	7.3732E-2 0.1424	6.6800E-2 0.0273	6.5547E-2 0.4210	4.8956E-2 0.6802	3.0554E-2
$d_2^{N,M}$ $q_2^{N,M}$	7.4012E-2 0.1518	6.6800E-2 0.0273	6.5547E-2 0.4210	4.8956E-2 0.6802	3.0554E-2

splitting systems with more components. Figure 3 displays the numerical solution at $T = 1$ for $\varepsilon = 10^{-4}$. Again, we clearly see the regular boundary layers at the outflow of the spatial domain.

The maximum errors and the numerical orders of convergence are calculated in the same way as for the first example and we use again the decomposition

19

Fig. 3. Components u_1 (left top), u_2 (right top) and u_2 (bottom) at $T = 1$ for $\varepsilon = 10^{-4}$ with $N = M = 32$
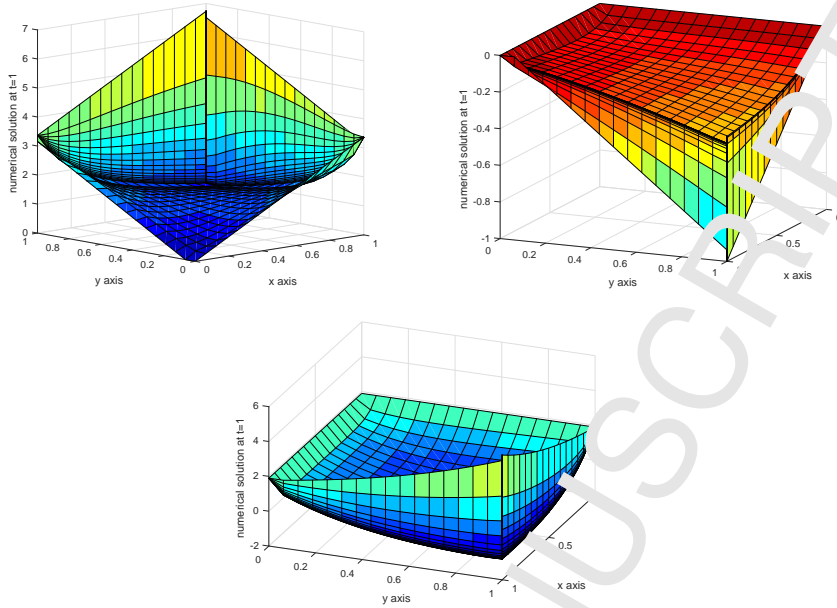
given in (34) for the right-hand side of the differential equation. Tables 7, 8 and 9 show the results for some values of ε for first, second and third component respectively. These results correspond to the use of improved boundary conditions according to (23). From them, we clearly observe the uniformly convergent behavior of the present algorithm which is almost first order and supports the theoretical results.

Table 7
Maximum errors and orders of convergence in **Example 3** for u_1

ε	N=16 M=8	N=32 M=16	N=64 M=32	N=128 M=64	N=256 M=128
2^{-6}	4.585?E-1	3.2635E-1	2.1155E-1	1.3000E-1	7.6284E-2
	0.4907	0.6254	0.7025	0.7690	
2^{-8}	4.584?E-1	3.3291E-1	2.1813E-1	1.3431E-1	7.8863E-2
	?.?616	0.6099	0.6997	0.7681	
2^{-10}	4.5655E-1	3.3331E-1	2.1954E-1	1.3536E-1	7.9518E-2
	0.4?39	0.6024	0.6977	0.7674	
2^{-12}	4.5591E-1	3.3325E-1	2.1978E-1	1.3558E-1	7.9649E-2
	0.4521	0.6005	0.6969	0.7674	
$\vdots$	...	...	...	...	...
	...	...	...	...	
2^{-42}	4.5567E-1	3.3321E-1	2.1985E-1	1.3565E-1	7.9684E-2
	0.4516	0.5999	0.6967	0.7675	
$d_1^{N,M}$	4.5855E-1	3.3331E-1	2.1985E-1	1.3565E-1	7.9684E-2
$q_1^{N,M}$	0.4602	0.6004	0.6967	0.7675	

20

Table 8
Maximum errors and orders of convergence in **Example 3** for u_2

ε	N=16 M=8	N=32 M=16	N=64 M=32	N=128 M=64	N=256 M=128
2^{-6}	6.6804E-2 0.2042	5.7987E-2 0.5545	3.9483E-2 0.6824	2.4603E-2 0.7396	1.4735E-2
2^{-8}	6.8721E-2 0.2353	5.8378E-2 0.5341	4.0315E-2 0.6694	2.5349E-2 0.7285	1.5299E-2
2^{-10}	7.1566E-2 0.2911	5.8489E-2 0.5276	4.0574E-2 0.6643	2.5602E-2 0.7252	1.5487E-2
2^{-12}	7.2293E-2 0.3049	5.8520E-2 0.5259	4.0643E-2 0.6630	2.5668E-2 0.7242	1.55?E-2
...	... ...	... ...	... ...	... ..	...
2^{-22}	7.2537E-2 0.3095	5.8531E-2 0.5254	4.0666E-2 0.6626	2.56?0E-? ?7239	1.5554E-2
$q_2^{N,M}$ $d_2^{N,M}$	7.2537E-2 0.3095	5.8531E-2 0.5254	4.0666E-2 0.6626	2.5690E-? ?7239	1.5554E-2

Table 9
Maximum errors and orders of convergence in **Example 3** for u_3

ε	N=16 M=8	N=32 M=16	N=64 M=32	N=128 M=64	N=256 M=128
2^{-6}	5.6305E-1 0.6271	3.6455E-1 0.6547	2.3??7E-1 0.?188	1.4070E-1 0.7718	8.2408E-2
2^{-8}	5.7665E-1 0.6251	3.7388E-1 0.6594	2.3671E-1 0.7278	1.4293E-1 0.7857	8.2910E-2
2^{-10}	5.7988E-1 0.6243	3.7619E-1 0.6610	2.3792E-1 0.7298	1.4346E-1 0.7915	8.2884E-2
2^{-12}	5.8067E-1 0.6241	3.7675E-1 0.66?3	2.3821E-1 0.7304	1.4358E-1 0.7586	8.4866E-2
...	. ...	... ...	... ...	... ...	...
2^{-22}	5.808?E-1 0.6?41	3.7693E-1 0.6615	2.3831E-1 0.7305	1.4362E-1 0.7411	8.5928E-2
$q_3^{N,M}$ $d_3^{N,M}$	5.809?E-1 0.6?41	3.7693E-1 0.6615	2.3831E-1 0.7305	1.4362E-1 0.7411	8.5928E-2

6 Conclusions

A numerical algorithm is proposed, analyzed and tested for solving two dimensional parabolic singularly perturbed weakly coupled systems of convection-diffusion type. Such method combines the standard upwind scheme on an appropriate spatial mesh and the fractional implicit Euler method, combined with a suitable splitting by directions and components of the spatial difference

21

operator. We prove that this method is uniformly convergent of first order in time and of almost first order in space. The chosen splitting technique means that only tridiagonal systems must be solved; therefore, the computational cost of the fully discrete algorithm is low in comparison with more classical implicit methods. Moreover, the order reduction of the method, related to the standard discretization of time dependent boundary data, can be ended in an easy way. Some numerical experiments are performed which show the main qualities of the algorithm.

Acknowledgements

References

[1] S. Bellew, E. O'Riordan, A parameter robust numerical method for a system of two singularly convection-diffusion equations, *Appl. Numer. Math.* **51** (2004) 171–186.

[2] C. Clavero, J.L. Gracia, Uniformly convergent additive schemes for 2D singularly perturbed parabolic systems of reaction-diffusion type, *Numer. Algorithms*, doi.org/10.1007/s11075-018-0518-y.

[3] C. Clavero, J.L. Gracia, J.C. Jorge, A uniformly convergent alternating direction HODIE finite difference scheme for 2D time dependent convection-diffusion problems, *IMA J. Numer. Anal.* **26** (2006) 155–172.

[4] C. Clavero, J.C. Jorge, Uniform convergence and order reduction of the fractional implicit Euler method to solve singularly perturbed 2D reaction-diffusion problems, *Appl. Math. Comp.* **287–88** (2016) 12–27.

[5] C. Clavero, J.C. Jorge, Solving efficiently one dimensional parabolic singularly perturbed reaction-diffusion systems: a splitting by components, *Appl. Math. Comp.* **287–88** (2016) 12–27.

[6] C. Clavero, J.C. Jorge, A multi-splitting method for two dimensional parabolic singularly perturbed systems of reaction-diffusion type, *J. Comp. Appl. Math* **344** (2018) 1–14.

[7] C. Clavero, J.C. Jorge, F. Lisbona, G.I. Shishkin, A fractional step method on a special mesh for the resolution of multidimensional evolutionary convection-diffusion problems, *Appl. Numer. Math.* **27 (3)** (1998) 211–231.

[8] A. Das, S. Natesan, Higher-order convergence with fractional-step method for singularly perturbed 2D parabolic convectiondiffusion problems on Shishkin mesh, *Comp. Math. Appl.* **75** (2018) 2387–2403.

[9] P.A. Farrell, A.F. Hegarty, J.J.H. Miller, E. O'Riordan, G.I. Shishkin, Robust Computational Techniques for Boundary Layers, Applied Mathematics, **16**. Chapman and Hall/CRC, (2000).

[10] R.B. Kellogg, T. Linss, M. Stynes, A finite difference method on layer-adapted meshes for an elliptic reaction-diffusion system in two dimensions, *Math. Comput.* **774** (2008) 2085–2096.

[11] R.B. Kellogg, N. Madden, M. Stynes, A parameter robust numerical method for a system of reaction-diffusion equations in two dimensions, *Numer. Methods Partial Differential Equations* **24** (2007) 312–334.

[12] O.A. Ladyzhenskaya, V.A. Solonnikov, and N.N. Uraltseva, Linear and Quasilinear Equations of Parabolic Type, Translations of Mathematical Monographs, **23**, American Mathematical Society, Providence, R.I. (1967).

[13] T. Linss, Analysis of an upwind finite-difference scheme for a system of coupled singularly perturbed convection-diffusion equations, *Computing* **79** (2007) 23–32.

[14] T. Linss, Analysis of a system of singularly perturbed convection-diffusion equations with strong coupling, *SIAM J. Numer. Anal.* **47 (3)** (2009) 1847–1862.

[15] T. Linss, M. Stynes, Numerical solution of systems of singularly perturbed differential equations, *Comput. Methods Appl. Math.* **9** (2009) 165–191.

[16] R. M. Priyadharshini, N. Ramanujam, A. Tamilsevan, Hybrid difference schemes for a system of singularly perturbed convection-diffusion equations, *J. Appl. Math. & Informatics* **27** (2009) 1001–1015.

[17] M.H. Protter, H.F.Weinberger, Maximum Principle in Differential Equations, Prentice-Hall, Englewood Cliffs, NJ (1967).

[18] H.G. Roos, C. Reibiger, Analysis of a strongly coupled system of two convection-diffusion equations with full layer interaction, *Z. Angew. Math. Mech.* **91** (2011) 537–543.

[19] H.G. Roos, M. Stynes, L. Tobiska, Robust numerical methods for singularly perturbed differential equations, Springer Series in Computational Mathematics, Berlin (2008).

[20] G.I. Shishkin, Approximation of systems of singularly perturbed elliptic reaction-diffusion equations with two parameters, *Comput. Math. Math. Phys.* **47** (2007) 797–828.

23